



## Original Article

## Use of waste water glass as silica supplier in synthesis of pure and Mg-doped lanthanum silicate powders for IT-SOFC application



C. Yamagata\*, D.R. Leme, S.R.H. Mello Castanho

*Materials Science and Technology Center, Nuclear and Energy Research Institute, Brazil*

## ARTICLE INFO

## Keywords:

Water glass  
Apatite-La silicate  
Synthesis  
Precipitation  
Sol gel  
SOFC  
Electrolyte

## ABSTRACT

Water glass in alkali solution ( $\text{Na}_2\text{SiO}_3/\text{NaOH}$ ) an abundant effluent, generated in the alkaline fusion of zircon sand, represents a potential silica source to be converted in useful silica technological application. Actually, the generation of energy by environmental-friendly method is one of the major challenges for researchers. Solid Oxide Fuel Cells (SOFC) is efficient and environmentally clean technique to energy production, since it converts chemical energy into electrical power, directly. Apatite-type lanthanum silicates are promising materials for application as an electrolyte in intermediate temperature SOFC (IT-SOFC) because of their higher ionic conductivity, in temperatures of range 600–700 °C, than conventional zirconia electrolytes. In this work, pure ( $\text{La}_{9.56}(\text{SiO}_4)_6\text{O}_{2.34}$ ) and Mg-doped ( $\text{La}_{9.8}\text{Si}_{5.7}\text{Mg}_{0.3}\text{O}_{26.4}$ ) lanthanum silicate were synthesized, from that rich effluent. Using the sol-gel followed by precipitation method, the single crystalline apatite phase of both silicates was obtained by thermal treatment at 900 °C of their precursors. Sintered ceramic samples reached density of higher than 90%.

## 1. Introduction

Recently, there is a major interest to develop efficient materials as electrolyte for SOFC [1–3] to lowering [4] the working temperature of the system. Ytria stabilized zirconia (YSZ); the conventional SOFC electrolyte operates in the temperature range 800–1000 °C with maximum oxide ion conductivity of  $\sim 0.1 \text{ S cm}^{-1}$  at 1000 °C [5]. This range of temperature [6] causes serious problems such as thermal and chemical durability of the material components sealing of the cell and material degradation and consequently the diminishing of the cell life.

Reduction of operating temperature of solid oxide fuel cells down to intermediate temperature (600–800 °C) gives significant advantages such as wider ranges of material selection, longer life and lower manufacturing costs. Development of solid electrolytes that display high ionic conductivity at low temperatures is one of the challenges to overcome to obtain intermediate temperature solid oxide fuel cells (IT-SOFCs) and for they become commercial scale.

Among the novel solid electrolytes, ceria-based ceramics (Gd-doped  $\text{CeO}_2$  (CGO)) have been considered as promising electrolytes for IT-SOFCs because of their high ionic conductivity compared with YSZ [7–9]. Similar to zirconia, ceria forms the fluorite which is a usual structure for electrolyte material for SOFCs. As well as zirconia, ceria is doped to increase its conductivity. Highest conductivity occurs by ion

doping, with the smallest size mismatch, such as gadolinium and samarium [10,11]. Doping with up to 20 mol%  $\text{Gd}_2\text{O}_3$  increases the ionic conductivity of Gd-doped  $\text{CeO}_2$  (CGO) that is more viable than that presented by traditional YSZ electrolytes in the lower temperature range [8,12]. Below 600 °C, comparing the conductivity of the most widely used ceria-based electrolyte,  $\text{Ce}_{1-x}\text{Gd}_x\text{O}_2$  (CGO) [13–15], with those of YSZ, the conductivities of CGO are consistently higher.

Rare earth silicates apatite-type structure in the general formula  $\text{RE}_{9.33+x}\text{Si}_6\text{O}_{26+1.5x}$  are a new class of oxide-ion conductors that have attracted considerable attention for use as solid electrolytes for IT-SOFCs [16,17] after researches made by Nakayama et al. [18]. Nakayama [18] revealed that the conductivity of the lanthanum-silicate-oxapatite (LSA) ceramics is higher than the conductivity of yttria stabilized zirconia ceramics below 600 °C. For instance, their characteristic oxide ion conductivity of  $4 \text{ mS cm}^{-1}$  at 500 °C is higher than that of a typical YSZ SOFC electrolyte that is  $1 \text{ mS cm}^{-1}$  at the same temperature [18,19]. Differently from YSZ electrolyte whose conductivity depends on oxide vacancies, LSA exhibit ionic conduction via interstitial conduction [20,21]. Among apatite rare-earth silicates, the lanthanum silicates, exhibit the highest values of oxide ion conductivity at intermediate temperatures ( $\text{La}_{10}\text{Si}_6\text{O}_{27}$ :  $\sigma = 4 \times 10^{-3} \text{ Scm}^{-1}$  at 500 °C) [22,23]. Lanthanum silicates with general formula  $\text{La}_{9.33+x}(\text{SiO}_4)_6\text{O}_{2+1.5x}$  ( $0 \leq x \leq 0.67$ ) are intensely studied compounds

\* Corresponding author.

E-mail address: [yamagata@ipen.br](mailto:yamagata@ipen.br) (C. Yamagata).<https://doi.org/10.1016/j.jeurceramsoc.2019.03.045>

Received 27 December 2018; Received in revised form 18 March 2019; Accepted 19 March 2019

Available online 20 March 2019

0955-2219/ © 2019 Elsevier Ltd. All rights reserved.

[23,24]. Those compounds exhibit high ionic conductivity and low activation energy values at intermediate temperatures (500–700 °C) [24,25]. They are considered as promising electrolytes for IT-SOFCs [26–28]. Lanthanum silicate has hexagonal crystal system similar to apatite type of calcium phosphate  $\text{Ca}_{10}(\text{PO}_4)_6\text{O}_2$ . The apatite-type lanthanum silicate established by Nakayama [23,24] is characterized by a high ionic conductivity, at an intermediate temperature, dominated by the interstitial migration mechanism [28,29]. This characteristic of conductivity mechanism offers the possibility to improve the LSA properties as fuel cell electrolyte. It is related with the wide range of substitution (doping) possibilities on the La and Si sites in apatite structure accommodating a range of ion sizes [30,31]. Studies of substituting La and Si sites and their effect on LSA conductivities were investigated [29,31–33]. It has observed that conductivity is very sensitive to the doping regulation and the cation/anion non-stoichiometry [32]. Studies of a wide range of dopants have been reported [34–37] both doping of rare earth site (Mg, Ca, Sr, Ba, Bi, Mn, Co, Ni, Cu) and Si site (Ge, Ti, P, B, Al, Ga, Mn, Co, Fe, Mg, Zn, Ni, Cu). Research on improvement in oxygen ionic conductivity by chemical doping revealed that magnesium is an effective element to increase ionic conductivity and those magnesium ions might substitute into not only the La ion sites but also Si ion sites [37,38]. Yoshioka has found that the conductivity of apatite-type lanthanum silicates is greatly enhanced by Mg doping; a doping level of 0.3 Mg for  $\text{La}_{10}\text{Si}_6\text{O}_{27}$  gave the highest conductivity [37]. The main effort to the actual application of LSA as IT-SOFCs electrolyte remains in the difficulty to prepare dense ceramics. High temperatures (1600–1800 °C) and prolonged time are required to obtain a relative density of 90% for LSA prepared by conventional solid state synthesis route [17,38,39]. Secondary phases, such as  $\text{LaSi}_2\text{O}_5$  and  $\text{La}_2\text{Si}_2\text{O}_7$  could also remain in the system. Those phases deteriorate the conductivity of the ceramic electrolyte [40]. To synthesize powders with higher sinterability, wet-chemical routes are suggested, such as; sol-gel [41,42], modified sol-gel [43,44], molten salt [45], freeze-drying [46], co-precipitation [47], acid citric [48] and hydrothermal [49] methods. In all methods, the main objective is to overcome the difficulties of achieving the single phase of apatite, free of secondary phases, and also the obtaining of high density ceramic from the synthesized powder. In this paper we report the preparation of pure lanthanum silicate  $\text{La}_{9.56}(\text{SiO}_4)_6\text{O}_{2.34}$  and Mg-doped lanthanum silicate,  $\text{La}_{9.8}\text{Si}_{5.7}\text{Mg}_{0.3}\text{O}_{26.4}$  by combining sol-gel and precipitation methods. Single phase of apatite was obtained in both synthesized lanthanum silicates powders by calcining at 900 °C, which temperature is relatively low comparing to the temperatures used by other methods. Ceramics with densities of higher than 90% have attained.

## 2. Experimental

Lanthanum oxide,  $\text{La}_2\text{O}_3$  (Aldrich 99.9%), MgO (Vetec 99.9%) and  $\text{Na}_2\text{SiO}_3$  solution (an effluent derived from alkali fusion procedure of zircon sand) [50] were used as the starting materials. The steps involved in the obtaining  $\text{Na}_2\text{SiO}_3$  solution are schematically showed in above reaction:



The transparent  $\text{Na}_2\text{SiO}_3$  solution contains approximately 2%  $\text{SiO}_2$  and 10% NaOH. It was used as Si supplier.  $\text{La}_2\text{O}_3$  and MgO were previously calcined at 800 °C in order to remove water and/or oxycarbonates and to determine the correct amount of those reagents. Dried  $\text{La}_2\text{O}_3$  or/and MgO were then dissolved in 6 M HCl to obtain a clear solution, which was used as La and Mg provider solution.

A previous calculated volume of 6 M HCl followed by Si and La and Mg precursor solutions (stoichiometric amounts to achieve the final composition  $\text{La}_{9.56}(\text{SiO}_4)_6\text{O}_{2.33}$  or  $\text{La}_{9.8}\text{Si}_{5.7}\text{Mg}_{0.3}\text{O}_{26.4}$ ) were added to the  $\text{Na}_2\text{SiO}_3$  solution with vigorous and constant stirring. The volume of the HCl is that of it is sufficient to attain high acid medium after its total

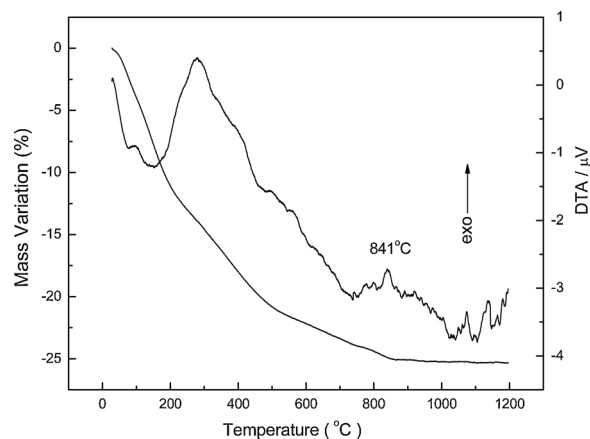


Fig. 1. TGA/DTA curves of dried  $\text{La}_{9.8}\text{Si}_{5.7}\text{Mg}_{0.3}\text{O}_{26.4}$ , of the sample LSM precursor gel.

addition. After complete adding, the mixture was kept at room temperature overnight. A clear gel of silica was formed. NaOH solution was then added to the gel, with vigorous and constant stirring, to give a final of pH 10.5 and precipitate La and Mg hydroxides. A turbid and milky sol was obtained. After that, the gel was filtered and washed with distilled water until no  $\text{Cl}^-$  was detected by  $\text{AgNO}_3$  test. The washed gel was dried overnight at 80 °C and calcined at 900 °C for 1 h to obtain apatite-type lanthanum powders,  $\text{La}_{9.56}(\text{SiO}_4)_6\text{O}_{2.33}$  or  $\text{La}_{9.8}\text{Si}_{5.7}\text{Mg}_{0.3}\text{O}_{26.4}$ , those samples were named LSI and LSM, respectively. The obtained powders were characterized by thermal analysis (TGA-DTA), X-ray diffraction (XRD), scanning electron microscopy (SEM) and specific surface area measurements (BET technique). As-synthesized apatite powders were uniaxially pressed into pellets under a pressure of 150 MPa and sintered at 1300 °C for 4 h in air. Bulk density was determined by Archimedes method in water.

## 3. Results and discussion

In order to determine the phase formation and transition temperatures, the dried precursor gel of LSM, was investigated by thermal analysis as shown in Fig. 1. The mass variation of 25%, observed between 25–865 °C, might be attributed to the dehydration process of the gel of silica,  $\text{La}(\text{OH})_3$  and  $\text{Mg}(\text{OH})_2$ . According to the DTA curve, an exothermic peak is observed at 841 °C, it may be attributed to the crystallization or formation of apatite-type  $\text{La}_{9.8}\text{Si}_{5.7}\text{Mg}_{0.3}\text{O}_{26.4}$  phase.

The XRD patterns obtained from the dried gel of the samples LSI and LSM, thermal treated at 900 °C for 1 h, are showed in Fig. 2.

From Fig. 2, it is observed that both samples present the same XRD spectra and the single phase apatite of lanthanum silicate was attained, confirming the crystallization peak observed at 841 °C in Fig. 1. Present thermal treatment conditions (900 °C for 1 h) of the powders compared to those presented by Cao et al. [51] are much lower. They prepared  $\text{La}_{9.67}\text{Si}_6\text{O}_{26.5}$  (LSO),  $\text{La}_{9.5}\text{Sr}_{0.5}\text{Si}_{5.5}\text{Fe}_{0.5}\text{O}_{26.5}$  (LSSFO) and  $\text{La}_{9.5}\text{Sr}_{0.5}\text{Si}_{5.5}\text{Al}_{0.5}\text{O}_{26.5}$  (LSSAO). As they were synthesized by solid state reaction route, the single phase of oxyapatite is very difficult to obtain and they are often contaminated with either  $\text{La}_2\text{SiO}_5$  or  $\text{La}_2\text{Si}_2\text{O}_7$  secondary phases. From XRD patterns of LSSFO powders calcined at 1000, 1100, 1200, 1300 and 1400 °C for 10 h in air,  $\text{La}_2\text{SiO}_5$  secondary phase was observed in XRD patterns of LSSFO. The intensity of the minor  $\text{La}_2\text{SiO}_5$  secondary phase decreases with the increase of the temperature of calcining and the same time the crystallinity of LSSFO oxyapatite is improved. From LSO, LSSAO and LSSFO powders calcined at 1300 °C for 10 h in air, the secondary phase  $\text{La}_2\text{SiO}_5$  was also observed in the all XRD patterns. However, the intensity of  $\text{La}_2\text{SiO}_5$  phase in the XRD patterns of LSSAO and LSSFO is very low, indicating a very small amount of  $\text{La}_2\text{SiO}_5$  second phase. The authors give explanation

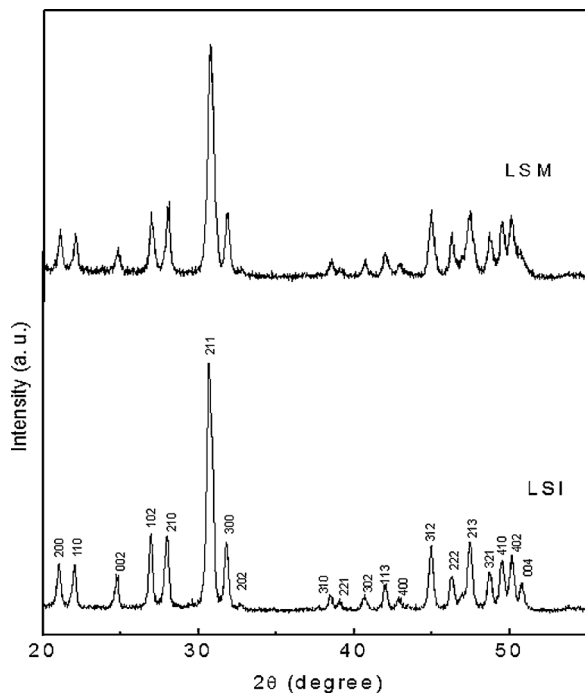


Fig. 2. XRD patterns obtained from the dried gel of the samples LSI and LSM, thermal treated at 900 °C for 1 h.

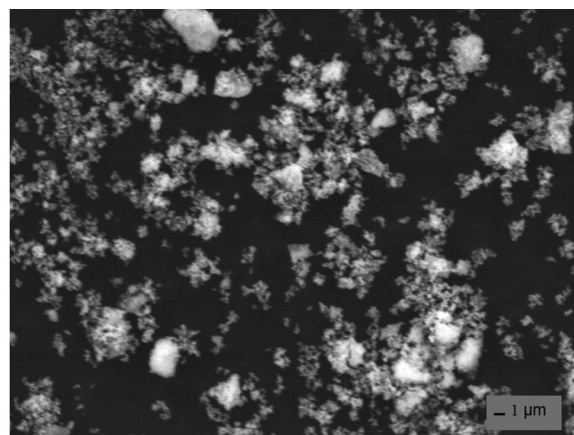
that co-doping of Sr and Al or Fe significantly prevents the formation of  $\text{La}_2\text{SiO}_5$  secondary phase.

Fig. 3 shows the SEM micrographs of the samples LSI and LSM calcined at 900 °C for 1 h.

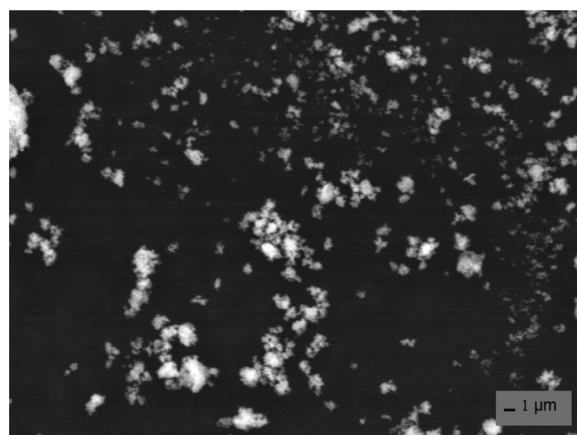
In Fig. 3 it can be observed that both samples presented similar morphology of the particles and agglomerates. The agglomerates look soft and porous. The particles are spherical like and sub-micron size. Specific surface area determined by the BET technique was of 14.4 and  $13.8 \text{ m}^2 \text{ g}^{-1}$ , for LSI and LSM, respectively. Fig. 4 shows XRD pattern of the sample LSM, sintered at 1300 °C for 4 h from powders calcined at 900 °C for 1 h. It is observed that the sintered ceramic presents the single phase of apatite and an increasing of the crystallinity. There is a narrowing of the peaks in Fig. 4 in comparison to the powder sample spectra, in Fig. 3. Sintered sample of LSI presented the identical XRD spectra showed in Fig. 4.

Fig. 5 shows the SEM micrographs of sintered surface of samples LSI (a) and LSM (b), obtained from powders calcined at 900 °C for 1 h, compacted to pellets and sintered at 1300 °C for 4 h.

In Fig. 5, it is observed a fine grained ceramic body in both micrographs, where the grains size up to 1  $\mu\text{m}$  is closely connected to each other. Some larger grains exhibit hexagonal appearance. The densification of the apatite materials by sintering treatment is advantageous for SOFC electrolytes applications. High density or low porosity is an important requirement for a SOFC electrolyte material [52]. The electrolyte density controls its electrical and mechanical properties [53] and, mainly, increasing of the density give an increasing its ionic conductivity. In the present work, high relative density of 94.92% and 95.55% were obtained for the ceramics of LSI and LSM respectively, after sintering at 1300 °C for 4 h. Reasonable large specific surface area and small particle size of the present synthesized powders might have promoted their reactivity and consequently their good sinterability to attain those high densities. Those sintering temperature and time are significantly lower than some reported results [26,53] in the literature, where temperatures exceeding 1600 °C are used. Yoshioka [26] prepared ceramic disks of apatite-type lanthanum silicates ( $\text{La}_x\text{Si}_6\text{O}_{1.5x+12}$  ( $8.96 \leq x \leq 10.57$ )) using sol-gel derived powders. He sintered first at 1600 °C and then 1750 °C. The disks were very porous after the first



(a)



(b)

Fig. 3. SEM micrographs of the samples LSI (a) and LSM (b) calcined at 900 °C for 1 h.

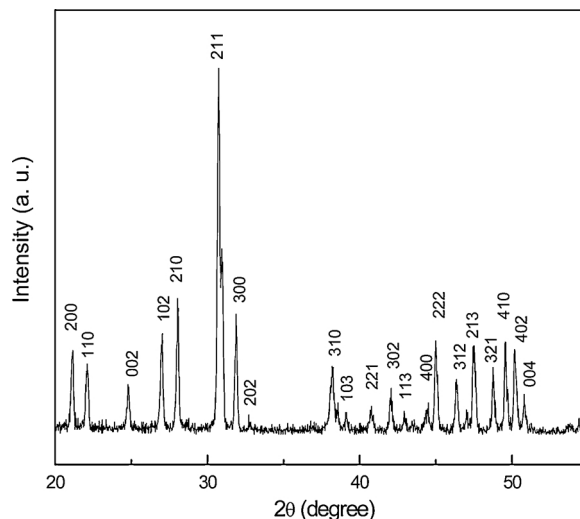
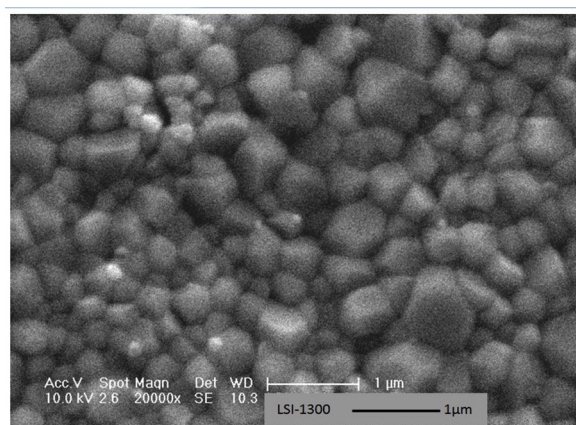
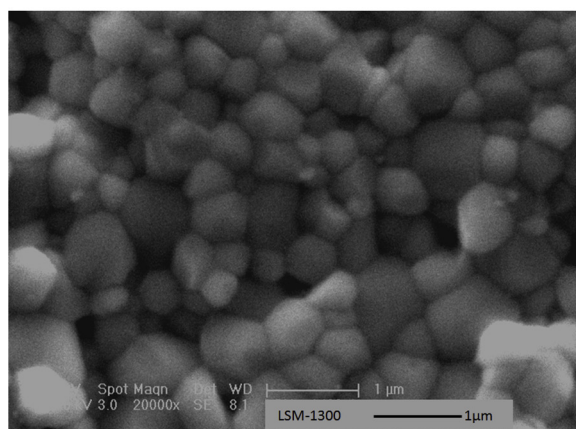


Fig. 4. XRD pattern of the sample LSM, sintered at 1300 °C for 4 h.

sintering at 1600 °C for 4 h. Then, the second sintering was performed at 1750 °C for 4 h to obtain dense ceramic disks having bulk densities of more than 85%.



(a)



(b)

Fig. 5. SEM micrographs of sintered surface of samples LSI (a) and LSM (b), obtained from powders calcined at 900 °C for 1 h, compacted to pellets and sintered at 1300 °C for 4 h.

#### 4. Conclusion

A new modified sol gel method to preparing lanthanum silicates ceramic powder was presented. Use of a waste solution of  $\text{Na}_2\text{SiO}_3$  is attractive and environmental-friendly for substituting of the usual high-cost TEOS (tetraethyl ortho silicate) as Si source. Apatite type lanthanum silicate powders were successfully synthesized by the proposed route, consisting of sol gel combined to precipitation technique. Crystalline apatite, without impurity phases, was attained by both samples,  $\text{La}_{9.56}(\text{SiO}_4)_6\text{O}_{2.33}$  (LSI) and  $\text{La}_{9.8}\text{Si}_{5.7}\text{Mg}_{0.3}\text{O}_{26.4}$  (LSM) after calcining the powders at 900 °C for 1 h. The good sinterability of the powders, due to their relatively large specific surface of approximately  $14 \text{ m}^2 \text{ g}^{-1}$  and small particle size, allowed the obtaining of ~95% high densities of ceramic body by sintering at 1300 °C for 4 h, from synthesized powders.

#### Acknowledgments

The authors gratefully acknowledge the financial support provided by The State of São Paulo Research Foundation (FAPESP – process 2018/10114-7) in the development of this work.

#### References

- [1] F. Ramadhani, M.A. Hussain, H. Mokhlis, S. Hajimolana, Optimization strategies for solid oxide fuel cell (SOFC) application: a literature survey, *Renew. Sustain. Energy Rev.* 76 (2017) 460–484.
- [2] G. Kaur, SOFC technology: its working and components, *Solid Oxide Fuel Cell Components*, Springer, 2016, pp. 79–122.
- [3] K. Kendall, M. Kendall, *High-temperature Solid Oxide Fuel Cells for the 21st Century: Fundamentals, Design and Applications*, Elsevier, 2015.
- [4] E.D. Wachsman, K.T. Lee, Lowering the temperature of solid oxide fuel cells, *Science* 334 (80) (2011) 935–939.
- [5] S.R. Hui, J. Roller, S. Yick, X. Zhang, C. Decès-Petit, Y. Xie, R. Maric, D. Ghosh, A brief review of the ionic conductivity enhancement for selected oxide electrolytes, *J. Power Sources* 172 (2007) 493–502.
- [6] N. Preux, A. Rolle, R.N. Vannier, Electrolytes and ion conductors for solid oxide fuel cells (SOFCs), *Funct. Mater. Sustain. Energy Appl.*, Elsevier, 2012, pp. 370–401.
- [7] N.P. Brandon, S. Skinner, B.C.H. Steele, Recent advances in materials for fuel cells, *Annu. Rev. Mater. Res.* 33 (2003) 183–213.
- [8] J.W. Fergus, Electrolytes for solid oxide fuel cells, *J. Power Sources* 162 (2006) 30–40.
- [9] M. Coduri, S. Checchia, M. Longhi, D. Ceresoli, M. Scavini, Rare Earth Doped Ceria: the complex connection between structure and properties, *Front. Chem.* 6 (2018).
- [10] H. Inaba, H. Tagawa, Ceria-based solid electrolytes, *Solid State Ion.* 83 (1996) 1–16.
- [11] K. Eguchi, T. Setoguchi, T. Inoue, H. Arai, Electrical properties of ceria-based oxides and their application to solid oxide fuel cells, *Solid State Ion.* 52 (1992) 165–172.
- [12] M.A.F. Öksüzömer, G. Dönmez, V. Sariboğa, T.G. Altınçekiç, Microstructure and ionic conductivity properties of gadolinia doped ceria ( $\text{GdxCe}_{1-x}\text{O}_{2-x/2}$ ) electrolytes for intermediate temperature SOFCs prepared by the polyol method, *Ceram. Int.* 39 (2013) 7305–7315.
- [13] M. Mogensen, D. Lybye, K. Kammer, N. Bonanos, Ceria revisited: Electrolyte or electrode material? *ECS Proc.* 2005 (2005) 1068–1074.
- [14] V.V. Kharton, F.M. Figueiredo, L. Navarro, E.N. Naumovich, A.V. Kovalevsky, A.A. Yaremchenko, A.P. Viskup, A. Carneiro, F.M.B. Marques, J.R. Frade, Ceria-based materials for solid oxide fuel cells, *J. Mater. Sci.* 36 (2001) 1105–1117.
- [15] D.H. Prasad, J.-W. Son, B.-K. Kim, H.-W. Lee, J.-H. Lee, A significant enhancement in sintering activity of nanocrystalline  $\text{CeO}_2$  9Gd0.1O1.95 powder synthesized by a glycine-nitrate-process, *J. Ceram. Process. Res.* 11 (2010) 176–183.
- [16] X. Ding, G. Hua, D. Ding, W. Zhu, H. Wang, Enhanced ionic conductivity of apatite-type lanthanum silicate electrolyte for IT-SOFCs through copper doping, *J. Power Sources* 306 (2016) 630–635.
- [17] J. Xiang, H.-Q. Chen, J.-H. Ouyang, Z.-G. Liu, J.-Y. Yu, F.-F. Wu, R.-D. Zhao, J. Shang, L. Liu, Stability and compatibility of lanthanum silicates electrolyte with standard cathode materials, *Ceram. Int.* 45 (2019) 6183–6189.
- [18] S. Nakayama, M. Higuchi, Electrical properties of apatite-type oxide ionic conductors RE<sub>9</sub> 33 (SiO<sub>4</sub>)<sub>6</sub>O<sub>2</sub> (RE = Pr, Nd and Sm) single crystals, *J. Mater. Sci. Lett.* 20 (2001) 913–915.
- [19] J. McFarlane, S. Barth, M. Swaffer, J.E.H. Sansom, P.R. Slater, Synthesis and conductivities of the apatite-type systems,  $\text{La}_{9.33+x}\text{Si}_{6-y}\text{M}_y\text{O}_{26+z}$  (M = Co, Fe, Mn) and  $\text{La}_{8}\text{Mn}_2\text{Si}_6\text{O}_{26}$ , *Ionics* (Kiel) 8 (2002) 149–154.
- [20] K. Kobayashi, Y. Matsushita, M. Tanaka, Y. Katsuya, C. Nishimura, Y. Sakka, Electrical conductivity and X-ray diffraction analysis of oxyapatite-type lanthanum silicate and neodymium silicate solid solution, *Solid State Ion.* 225 (2012) 443–447.
- [21] K. Kobayashi, T.S. Suzuki, T. Uchikoshi, Y. Sakka, Magnesium ion distribution and defect concentrations of MgO-doped lanthanum silicate oxyapatite, *Solid State Ion.* 258 (2014) 24–29.
- [22] S. Nakayama, T. Kageyama, H. Aono, Y. Sadaoka, Ionic conductivity of lanthanoid silicates,  $\text{Ln}_{10}(\text{SiO}_4)_6\text{O}_3$  (Ln = La, Nd, Sm, Gd, Dy, Y, Ho, Er and Yb), *J. Mater. Chem.* 5 (1995) 1801–1805.
- [23] S. Nakayama, M. Sakamoto, Electrical properties of new type high oxide ionic conductor RE<sub>10</sub>Si<sub>6</sub>O<sub>27</sub> (RE = La, Pr, Nd, Sm, Gd, Dy), *J. Eur. Ceram. Soc.* 18 (1998) 1413–1418.
- [24] S. Nakayama, H. Aono, Y. Sadaoka, Ionic Conductivity of  $\text{Ln}_{10}(\text{SiO}_4)_6\text{O}_3$  (Ln = La, Nd, Sm, Gd and Dy), *Chem. Lett.* 24 (1995) 431–432.
- [25] D. Marrero-López, M.C. Martín-Sedeño, J. Peña-Martínez, J.C. Ruiz-Morales, P. Núñez, M.A.G. Aranda, J.R. Ramos-Barrado, Evaluation of apatite silicates as solid oxide fuel cell electrolytes, *J. Power Sources* 195 (2010) 2496–2506.
- [26] H. Yoshioka, Oxide ionic conductivity of apatite-type lanthanum silicates, *J. Alloys Compd.* 408 (2006) 649–652.
- [27] W. Gao, W.-Y. Li, H.-L. Liao, C. Coddet, Electrical properties of atmospheric plasma-sprayed  $\text{La}_{10}(\text{SiO}_4)_6\text{O}_3$  electrolyte coatings, *J. Therm. Spray Technol.* 20 (2011) 888–891.
- [28] E. Béchade, O. Masson, T. Iwata, I. Julien, K. Fukuda, P. Thomas, E. Champion, Diffusion path and conduction mechanism of oxide ions in apatite-type lanthanum silicates, *Chem. Mater.* 21 (2009) 2508–2517.
- [29] L. León-Reina, J.M. Porras-Vázquez, E.R. Losilla, M.A.G. Aranda, Interstitial oxide positions in oxygen-excess oxy-apatites, *Solid State Ion.* 177 (2006) 1307–1315.
- [30] A. Najib, J.E.H. Sansom, J.R. Tolchard, P.R. Slater, M.S. Islam, Doping strategies to optimise the oxide ion conductivity in apatite-type ionic conductors, *Dalton Trans.* (2004) 3106–3109.
- [31] H. Yoshioka, Enhancement of ionic conductivity of apatite-type lanthanum silicates doped with cations, *J. Am. Ceram. Soc.* 90 (2007) 3099–3105.
- [32] V.V. Kharton, A.L. Shaula, M.V. Patrakeev, J.C. Waerenborgh, D.P. Rojas, N.P. Vyshatko, E.V. Tsipis, A.A. Yaremchenko, F.M.B. Marques, Oxygen ionic and electronic transport in apatite-type solid electrolytes, *J. Electrochem. Soc.* 151 (2004) A1236–A1246.
- [33] E. Kendrick, M.S. Islam, P.R. Slater, Developing apatites for solid oxide fuel cells: insight into structural, transport and doping properties, *J. Mater. Chem.* 17 (2007) 3104–3111.
- [34] J.R. Tolchard, P.R. Slater, M.S. Islam, Insight into doping effects in apatite silicate ionic conductors, *Adv. Funct. Mater.* 17 (2007) 2564–2571.
- [35] S. Lambert, A. Vincent, E. Bruneton, S. Beaudet-Savignat, F. Guillet, B. Minot,

- F. Bouree, Structural investigation of La<sub>9</sub> 33Si<sub>6</sub>O<sub>26</sub>-and La<sub>9</sub>AE<sub>3</sub>Si<sub>6</sub>O<sub>26</sub>+  $\delta$ -doped apatites-type lanthanum silicate (AE = Ba, Sr and Ca) by neutron powder diffraction, *J. Solid State Chem.* 179 (2006) 2602–2608.
- [36] H. Yoshioka, Y. Nojiri, S. Tanase, Ionic conductivity and fuel cell properties of apatite-type lanthanum silicates doped with Mg and containing excess oxide ions, *Solid State Ion.* 179 (2008) 2165–2169.
- [37] H. Yoshioka, High oxide ion conductivity in Mg-doped La<sub>10</sub>Si<sub>6</sub>O<sub>27</sub> with apatite-type structure, *Chem. Lett.* 33 (2004) 392–393.
- [38] Y. Nojiri, S. Tanase, M. Iwasa, H. Yoshioka, Y. Matsumura, T. Sakai, Ionic conductivity of apatite-type solid electrolyte material, La<sub>10</sub> – XBaXSi<sub>6</sub>O<sub>27</sub> – X/2 (X = 0–1), and its fuel cell performance, *J. Power Sources* 195 (2010) 4059–4064.
- [39] E. Béchade, I. Julien, T. Iwata, O. Masson, P. Thomas, E. Champion, K. Fukuda, Synthesis of lanthanum silicate oxyapatite materials as a solid oxide fuel cell electrolyte, *J. Eur. Ceram. Soc.* 28 (2008) 2717–2724.
- [40] S. Celerier, C. Laberty-Robert, F. Ansart, C. Calmet, P. Stevens, Synthesis by sol–gel route of oxyapatite powders for dense ceramics: Applications as electrolytes for solid oxide fuel cells, *J. Eur. Ceram. Soc.* 25 (2005) 2665–2668.
- [41] Y. Ma, N. Fenineche, O. Elkedim, M. Moliere, H. Liao, P. Briois, Synthesis of apatite type La<sub>10</sub> – xSrxSi<sub>6</sub>O<sub>27</sub> – 0.5 x powders for IT-SOFC using sol–gel process, *Int. J. Hydrogen Energy* 41 (2016) 9993–10000.
- [42] E. Jothinathan, K. Vanmeensel, J. Vleugels, O. Van der Biest, Synthesis of nanocrystalline apatite type electrolyte powders for solid oxide fuel cells, *J. Eur. Ceram. Soc.* 30 (2010) 1699–1706.
- [43] A.M. Misso, D.R. Elias, F. dos Santos, C. Yamagata, Low temperature synthesis of lanthanum silicate apatite type by modified sol gel process, *Adv. Mater. Res., Trans Tech Publ* (2014) 143–148.
- [44] C. Yamagata, D.R. Elias, M.R.S. Paiva, A.M. Misso, S.R.H.M. Castanho, Facile preparation of apatite-type lanthanum silicate by a new water-based sol–gel process, *Mater. Res. Bull.* 48 (2013) 2227–2231.
- [45] B. Li, J. Liu, Y. Hu, Z. Huang, Preparation and characterization of La<sub>9</sub> 33Si<sub>6</sub>O<sub>26</sub> powders by molten salt method for solid electrolyte application, *J. Alloys Compd.* 509 (2011) 3172–3176.
- [46] A. Chesnaud, G. Dezanneau, C. Estournès, C. Bogicevic, F. Karolak, S. Geiger, G. Geneste, Influence of synthesis route and composition on electrical properties of La<sub>9</sub>. 33 + xSi<sub>6</sub>O<sub>26</sub> + 3x/2 oxy-apatite compounds, *Solid State Ion.* 179 (2008) 1929–1939.
- [47] P. Jena, S. Jayasubramanian, P.K. Patro, R.K. Lenka, A. Sinha, P. Muralidharan, E.S. Srinadhu, N. Satyanarayana, Structural characterization, electrical conductivity and open circuit voltage studies of the nanocrystalline La<sub>10</sub>Si<sub>6</sub>O<sub>27</sub> electrolyte material for SOFCs, *Appl. Phys. A* 124 (2018) 125.
- [48] T. Yang, H. Zhao, M. Fang, K. Świerczek, J. Wang, Z. Du, A new family of Cu-doped lanthanum silicate apatites as electrolyte materials for SOFCs: Synthesis, structural and electrical properties, *J. Eur. Ceram. Soc.* 39 (2019) 424–431.
- [49] P. Jena, P.K. Patro, A. Sinha, R.K. Lenka, A.K. Singh, T. Mahata, P.K. Sinha, Hydrothermal synthesis and characterization of an apatite type lanthanum silicate ceramic for solid oxide fuel cell electrolyte applications, *Energy Technol.* 6 (2018) 1739–1746.
- [50] C. Yamagata, J.B. Andrade, V. Ussui, N.B. de Lima, J.O.A. Paschoal, High purity zirconia and silica powders via wet process: alkali fusion of zircon sand, *Mater. Sci. Forum* (2008) 771–776. *Trans Tech Publ.*
- [51] X.G. Cao, S.P. Jiang, Effect of Sr and Al or Fe co-doping on the sinterability and conductivity of lanthanum silicate oxyapatite electrolytes for solid oxide fuel cells, *Int. J. Hydrogen Energy* 39 (2014) 19093–19101.
- [52] M. Ghatee, M.H. Shariat, J.T.S. Irvine, Investigation of electrical and mechanical properties of 3YSZ/8YSZ composite electrolytes, *Solid State Ion.* 180 (2009) 57–62.
- [53] R.J.M. Toja, N.M. Rendtorff, E.F. Aglietti, T. Uchikoshi, Y. Sakka, G. Suárez, Influence of the porosity caused by incomplete sintering on the mechanical behaviour of lanthanum silicate oxyapatite, *Ceram. Int.* 44 (2018) 14348–14354.